Supporting Information

Protonation Regulates the Triplet State Decay of 6-Thioguanosine

Dongyu Li,[1] Yan Liu,[2] Shuyi Yan,[2] Qian Zhou,[2] Zhuoran Kuang,[1] Hongmei Zhao,[1] Yang Li,[1] Jialong Jie,[2] Di Song,*[1] Hongmei Su,*[2]*

1. State Key Laboratory of Information Photonic and Optical Communications, and School of Physical Science and Technology, Beijing University of Posts and Telecommunications (BUPT), Beijing 100876, P. R. China

2. College of Chemistry, Beijing Normal University, Beijing 100875, P. R. China

AUTHOR INFORMATION

Corresponding Author

* Jialong Jie E-mail: jialong@bnu.edu.cn
* Di Song E-mail: songdi@bupt.edu.cn
* Hongmei Su E-mail: hongmei@bnu.edu.cn

Contents

S1. Materials and Methods

Materials. 6-thioguanosine (6tGuo, 98%) was purchased from TargetMol and used without further purification. The 6tGuo was dissolved in 10 mM phosphate buffer solutions at pH 7.0 and 1.5, repsectively. By monitoring the absorbance at 350 nm and 355 nm in the UV-vis spectrum, the extinction coefficients of 6tGuo were determined to be ~ 9.1×10^3 M^{-1} cm^{-1} and ~ 3.7×10^3 M^{-1} cm^{-1}, respectively, while those of $6tGuoH^+$ were ~ 1.6×10^4 M^{-1} cm^{-1} and ~ 1.2×10^4 M^{-1} cm^{-1}.

Steady-State UV Absorption Spectra and Steady-State Emission Spectra. The steady-state UV absorption spectra were measured using a double-beam spectrometer (model U-3010, Hitachi). Each measurement was collected from 200 to 800 nm at a scan rate of 600 nm/min. Fluorescence spectra were measured on a steady-state emission spectrometer (F4600, Hitachi) at the excitation wavelength. All measurements were performed in 1 cm quartz cuvettes under air conditions at ambient temperature.

Time-Resolved Laser Flash Photolysis. Time-resolved laser flash photolysis (LFP) was used to measure the transient UV−vis absorption spectra.[1, 2] Briefly, an Edinburgh LP980 spectrometer (Edinburgh Instruments, UK) is synchronized with a commercial Nd:YAG laser (Lab 170, Spectral Physics Inc.). The excitation wavelength is 355 nm (1 Hz, fwhm ≈ 7 ns, 10 mJ/pulse). A monochromator equipped with a photomultiplier was used to collect the spectra with a range from 300 to 700 nm. The data were transferred to a personal computer after the signals from the photomultiplier were displayed and recorded as a function of time on a 100 MHz (1.25 Gs/s sampling rate) oscilloscope (Tektronix, TDS 3012C). Data were analyzed by the online software of the LP980 spectrophotometer.

Femtosecond Transient Absorption Spectra. The femtosecond transient absorption spectra were measured using a femtosecond transient absorption spectrometer (Harpia-TA, Light Conversion). The fundamental pulses (800 nm, 40 fs, 100 nJ, 1 kHz) were generated with a Ti:Sapphire laser system (Coherent Astrella) and

split by a beam splitter to generate the pump and probe beams. A small fraction of the fundamental pulses was sent to a computer-controlled optical delay line and then focused onto a CaF_2 plate to generate the white light continuum probe beam. The rest of the fundamental pulses were sent to the optical parametric amplifier (TOPAS-C, Coherent Inc.) to generate the 350 nm pump beam, which was chopped at 500 Hz. To avoid anisotropic signals, the polarizations of pump and probe beams were set to the magic angle (54.7°) in all measurements. The focused signal and pump beams were overlapped into a fused silica cuvette with a 1 mm beam path length, and control the steady-state absorbance of $6tGuoH^+$ at a wavelength of 350 nm to be 1. The frequent movement of the electrically driven sample holder ensures that the sample in the probed volume was continuously renewed to avoid re-excitation of the excited volume by successive laser pulses, similar to the function of a magnetic stirrer. The differential absorbance ΔA (t, λ) obtained from the femtosecond transient absorption spectra as a function of wavelength and time delay was analyzed using the Glotaran and CarpetView program.[3, 4]

Quantum Chemical Calculations. Quantum chemical calculations involving 6tGuo were performed with an anti-C2'-endo sugar conformation, which has been well elaborated in previous research.[5] As for the structure of $6tGuoH^+$, we conducted geometric optimizations on a set of candidate structures. When selecting these candidate structures, we considered the favorable protonation sites (N7 and N3), base orientations (anti and syn), and sugar ring conformations (C2′-endo and C3′-endo), as shown in Figure S1. The structural optimization calculations employed the extended hybrid density functional theory (X3LYP)[6] and the standard basis set 6-311++G**[7, 8] . This level of theory was chosen for its good balance of computational efficiency and accuracy at a moderate computational cost. DFT methods reliably describe the ground-state structures and stereoconformations of such nucleoside systems, and thus we first used this approach to determine the ground-state geometry.[9, 10] Frequency analysis was performed to determine the stationary points. The Gibbs free energies used for stability comparison incorporated zero-point energy corrections. At the same level of theory, the polarizable continuum model (PCM) was used to simulate the bulksolvent effects.[11] The calculation results showed that among all the candidate structures, the most stable

one was the N7-protonated form with an anti-C3'-endo sugar conformation. This is consistent with the protonation site and stereoconformation of the $GuoH^+$,[12] which is the parent molecule of $6tGuoH^+$.

As has been demonstrated in recent studies, incorporating explicit solvent effects is crucial for achieving an accurate description of the excitation energies in DNA bases and their thio-derivatives.[13, 14] To this end, in addition to accounting for bulk solvent effects, we strategically included explicit water molecules at sites where the bases are likely to form hydrogen bonds with water molecules in the calculations of vertical excitation energies, similar to our prior work treated with guanine base.[15] We reoptimized the N7-protonated form of $6tGuoH^+$ with an anti-C3'-endo sugar conformation using the 5-water-molecule microhydrated model at the PCM/X3LYP/6-311++G** level of theory, which is shown in Figure S2. Time-dependent density functional theory (TD-DFT) calculations were then performed at the same theoretical level on the newly obtained optimized configuration. Ten excited states were considered in the calculations. The Multiwfn software was used to visualize the vertical excitation energies, oscillator strengths, and transition properties.[16] Similar calculations were conducted for the neutral 6tGuo to obtain the vertical excitation energies. The above quantum chemical calculations were carried out using the Gaussian 16 software package.[17]

To unravel the deactivation pathways associated with intrinsic triplet lifetimes of 6tGuo and $6tGuoH^+$, we optimized their stationary geometries and conical intersections across the five lowest-lying electronic states (S_0, S_1, S_2, T_1, and T_2) using the state-averaged complete active space self-consistent field (CASSCF) method with the 6-31G** basis sets.[18-20] This approach was adopted to avoid biasing the relative energies of excited states, which are sensitive to the initial placement of explicit water molecules, and to properly account for the multiconfigurational character of the wavefunction near the crossing point. For both $6tGuoH^+$ and 6tGuo, we utilized identical active spaces. Each active space comprised 12 electrons in 10 orbitals, including five π and four π^* orbitals and a sulfur lone-pair orbital. The graphical depictions of these active orbitals are presented in Figure S4 and Figure S5. To validate the nature of the stationary points

obtained from the CASSCF optimization, frequency calculations were performed at the same theoretical level. To consider dynamic electron correlation, the relative excitation energies of their T_1 states and the T_1/S_0 crossing points were further determined through the second-order perturbation theory (CASPT2) at the same basis set level.[21, 22] In CASPT2 calculations, an imaginary level shift of 0.3 a.u. and the default IPEA shift of 0.25 a.u. are used. The CASPT2//CASSCF calculations are performed by using the MOLPRO 2012.1 package.[23]

S2. Supplementary Table Information

Table S1. Vertical excitation energies and Oscillator strengths for 6tGuo and $6tGuoH^+$ calculated using the 5-water-molecule microhydrated model calculated at the PCM/X3LYP/6-311++G** level of theory. Oscillator strengths are provided in parentheses.

State	6tGuo (eV)	$6tGuoH^+$ (eV)
S_2 ($\pi\pi_{cs}^*$)	3.69（0.64）	3.60（0.57）
S_1 ($n_s\pi_{cs}^*$)	3.44（0.00）	3.34（0.00）
T_3 ($\pi\pi_{cs}^*$)	3.84	3.68
T_2 ($n_s\pi_{cs}^*$)	3.25	3.13
T_1 ($\pi\pi_{cs}^*$)	2.72	2.59

Table S2. Triplet decay properties of 6tGuo and $6tGuoH^+$ under various concentrations and in their intrinsic states.

	6tGuo	$6tGuoH^+$
$\tau_{200\mu M}$/μs	0.5 ± 0.1	2.0 ± 0.1
$\tau_{100\mu M}$/μs	0.7 ± 0.1	3.6 ± 0.1
$\tau_{50\mu M}$/μs	1.0 ± 0.1	6.0 ± 0.1
$\tau_{25\mu M}$/μs	1.1 ± 0.1	7.9 ± 0.1
τ_0/μs	1.3 ± 0.1	15.5 ± 1.8
k_{SQ}/10^9 $M^{-1}s^{-1}$	5.7 ± 0.4	2.2 ± 0.1

S3. Supplementary Quantum Calculations

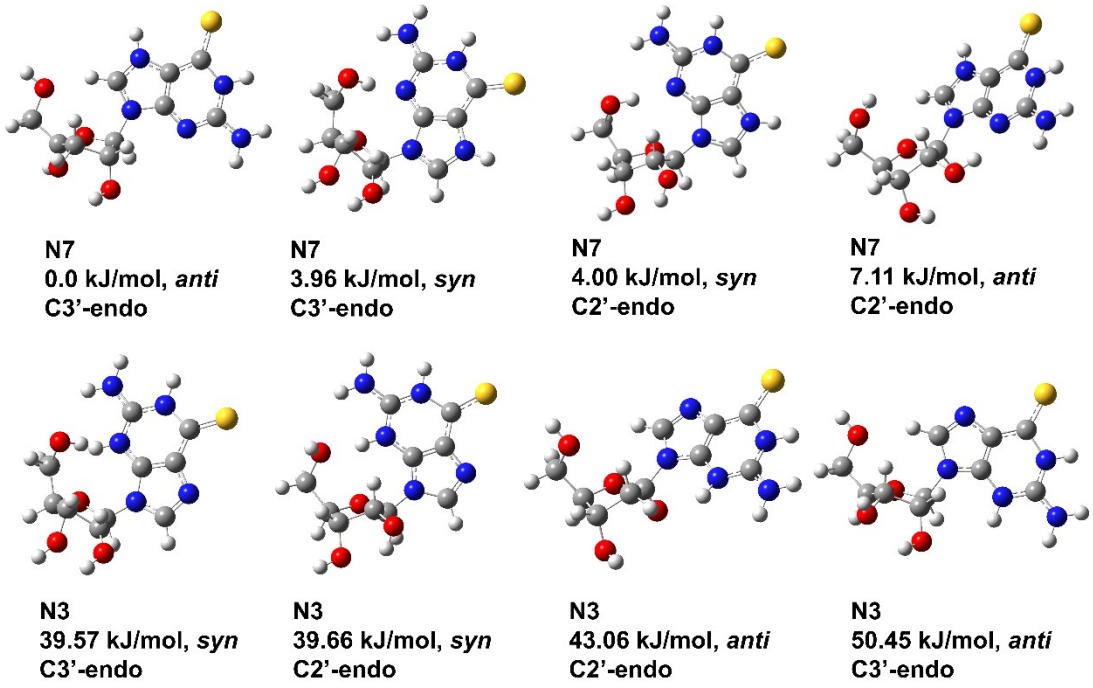

Figure S1. PCM/X3LYP/6-311++G** optimized geometries of the most stable N7 and N3 protonated conformers of the 6tGuoH$^+$. Protonation sites, nucleobase orientations (italicized font), sugar ring conformations, and PCM/X3LYP/6-311++G** relative Gibbs energy are given.

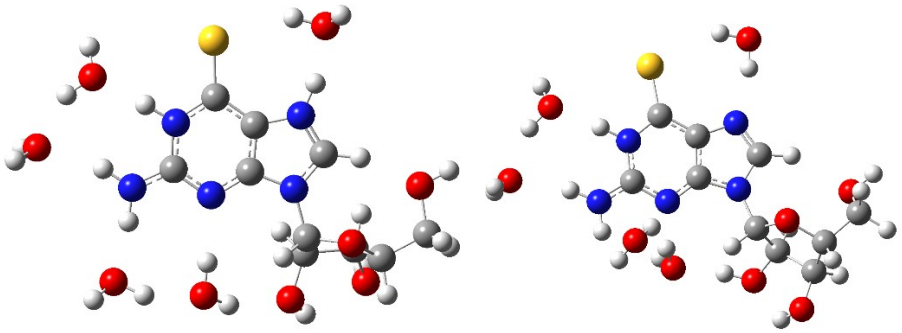

Figure S2. Optimized ground state structures of $6tGuoH^+$ and 6tGuo calculated using the 5-water-molecule microhydrated model at the PCM/X3LYP/6-311++G** level of theory.

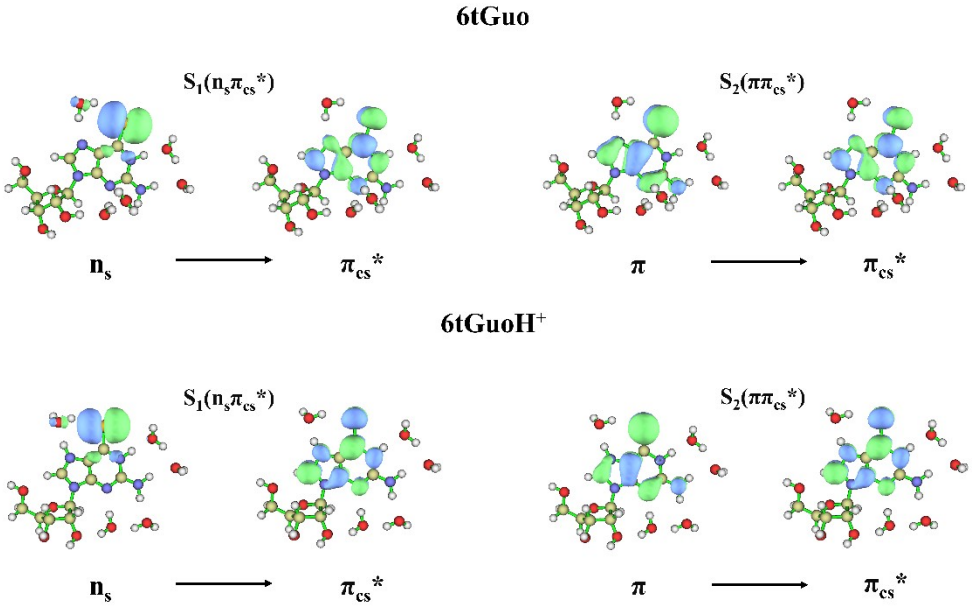

Figure S3. The molecular orbitals present a character of electronic transitions in the Franck-Condon region of 6tGuo and $6tGuoH^+$ using the 5-water-molecule microhydrated model calculated at the PCM/X3LYP/6-311++G** level of theory.

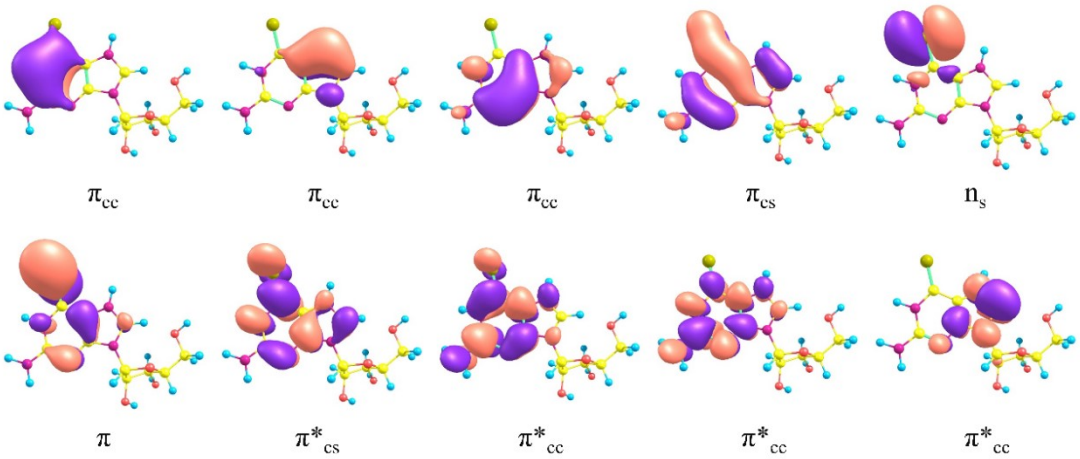

Figure S4. Graphical representation of $6tGuoH^+$ active orbitals for the CASSCF and CASPT2 calculations.

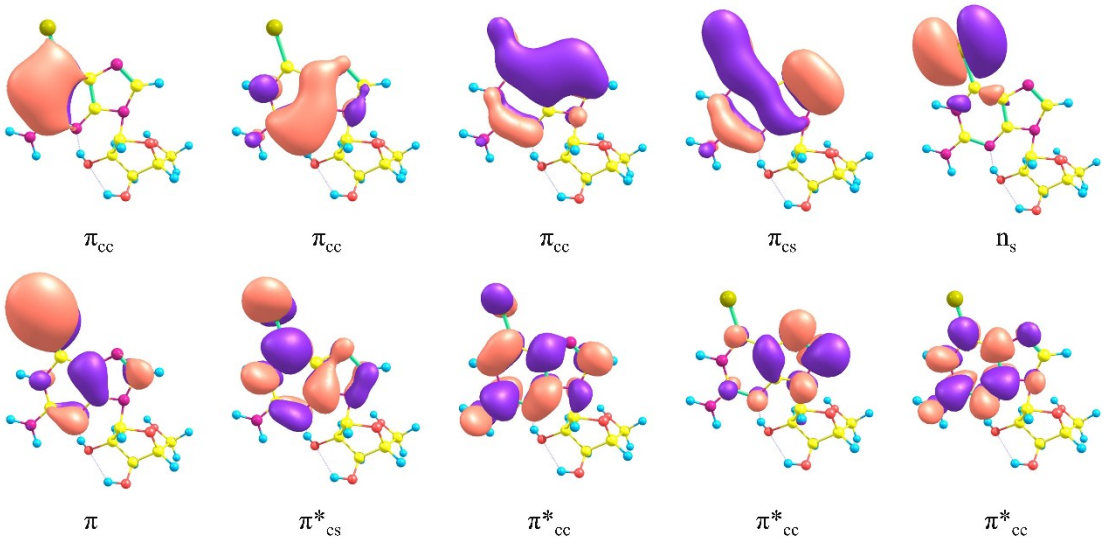

Figure S5. Graphical representation of 6tGuo active orbitals for the CASSCF and CASPT2 calculations.

S4. Supplementary Transient Absorption Spectra

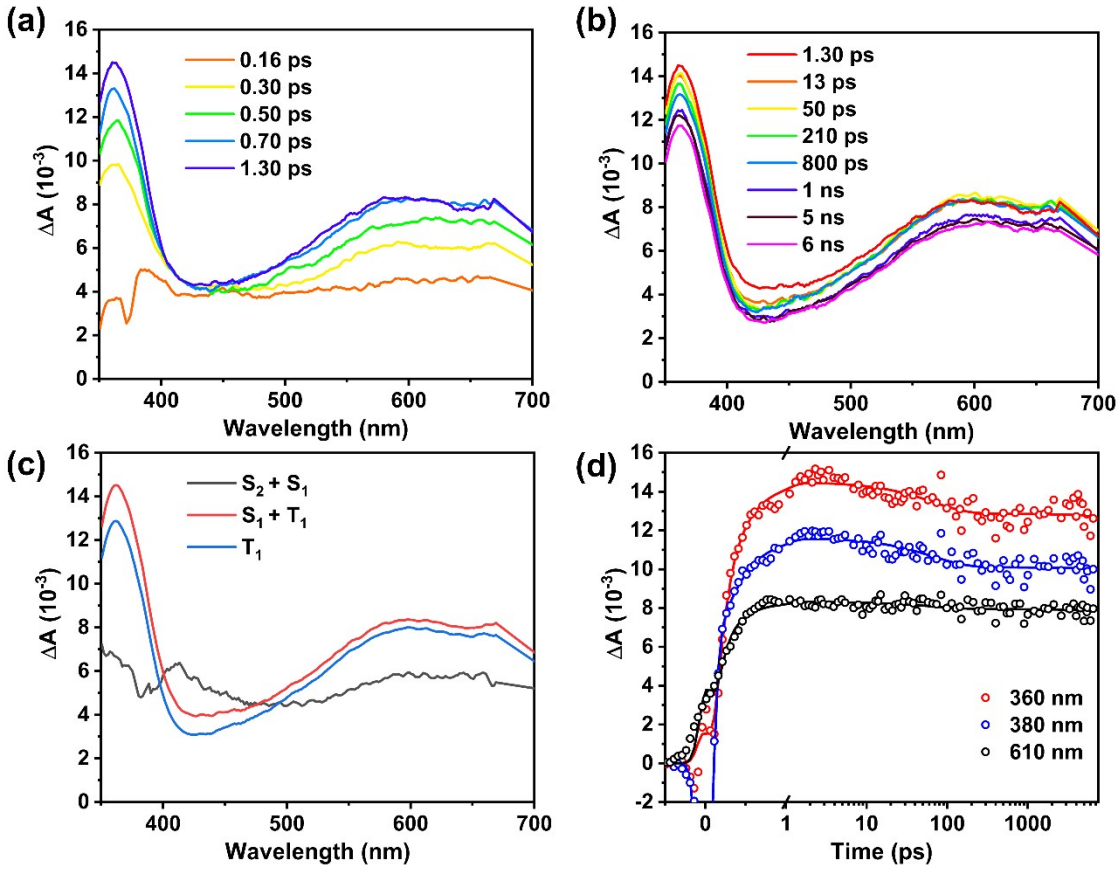

Figure S6. (a,b) The femtosecond time-resolved UV-vis absorption spectra of 6tGuo excited at 350 nm in PBS at pH 7.0, with the spectra at different time scales extracted. (c) The evolution-correlation difference spectrum of 6tGuo obtained from global fitting. (d) The representative decay signals of 6tGuo. Best global-fit curves are shown by solid lines.

We revisited the femtosecond transient absorption (fs-TA) spectra of 6tGuo in PBS at pH 7.0, extending the time window to 7 nanoseconds. Figure S6a and S6b show the spectra at different time delays, consistent with previous work.[5, 24] At early delays, two excited-state absorption (ESA) bands at 370 nm and 600 nm are observed, reaching maximum intensity at 1.3 ps. After rapid decay to ~210 ps, these bands decay more slowly, maintaining significant optical density at 6 ns, indicating their assignment to the long-lived T_1 triplet state.

To obtain kinetic information and verify the spectral assignments, we fitted the data with a sequential model using two exponential functions and a time-independent constant. The time constants τ_1 = 0.29 ps and τ_2 = 61 ps were obtained. The τ_1 value closely matches the 0.31 ps reported by Reichardt et al.,[5] supporting their assignment of τ_1 as reflecting the combination of internal conversion (IC) from S_2 to S_1 and intersystem crossing (ISC) to T_1. The τ_2 value of 61 ps also aligns with their 80 ps result, reflecting the combined effect of IC from S_1 to the ground state and solvent dynamics. The evolution-associated difference spectra (EADS) shows that T_1 and (T_1+S_1) exhibit similar spectral features, consistent with the experimental spectra (Figure S6c). The kinetic trace fitting (Figure S6d) reveals a pronounced picosecond decay, validating the global fitting model and providing a reliable reference for fs-TA measurements of 6tGuoH$^+$.

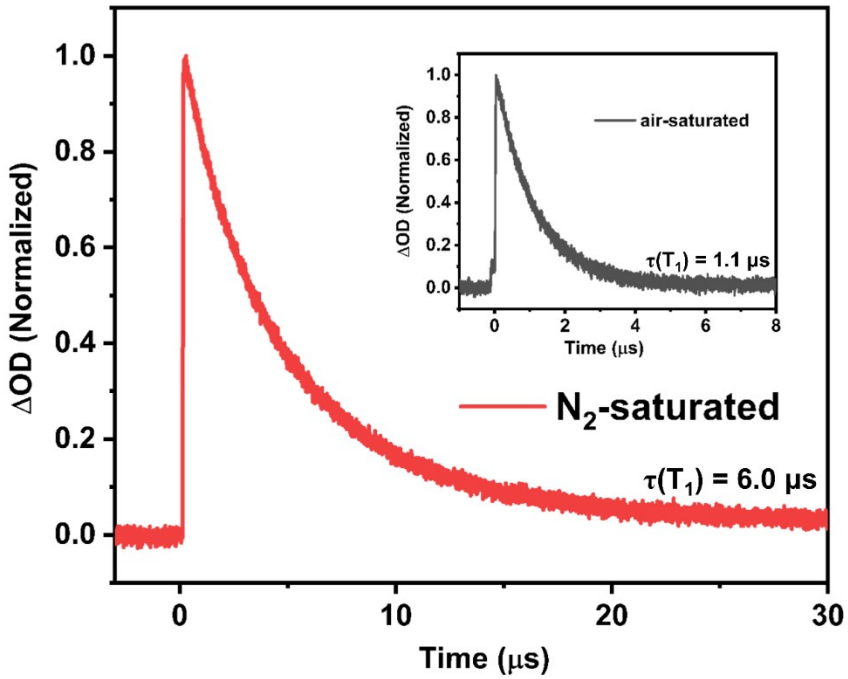

Figure S7. Under N_2-saturated conditions, a trace of triplet absorption for 50 μM 6tGuoH$^+$ in PBS at pH 1.5 was detected at 600 nm with an excitation wavelength of 355 nm. The inset depicts the trace under air-saturated conditions with identical sample (50 μM 6tGuoH$^+$) and detection (600 nm) conditions.

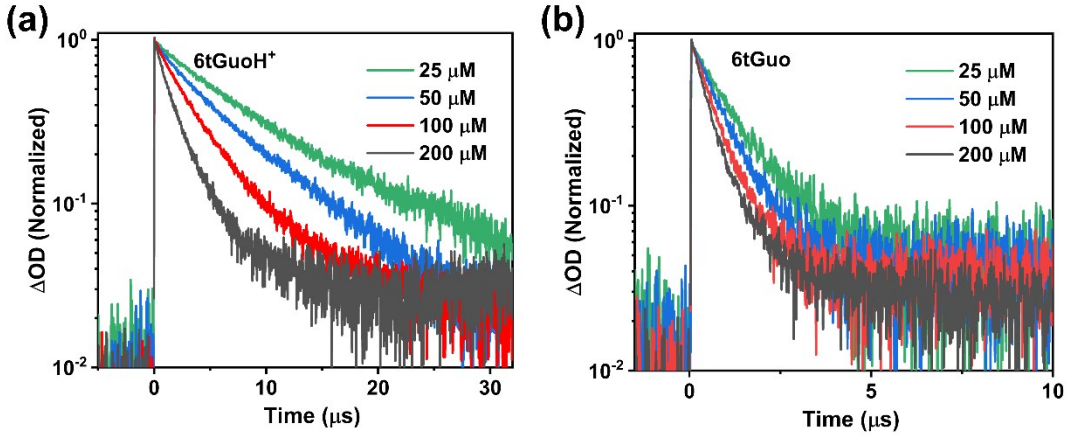

Figure S8. Triplet decay kinetics curves of 6tGuoH$^+$ (a) and 6tGuo (b) at different concentrations monitored at 600 nm under N_2-saturated conditions, with a logarithmic scale for the y-axis. The plateau in the transient signals is attributed to a longer-lived species (possibly products of triplet-ground state collisions), whose decay is much slower than that of the triplet state.

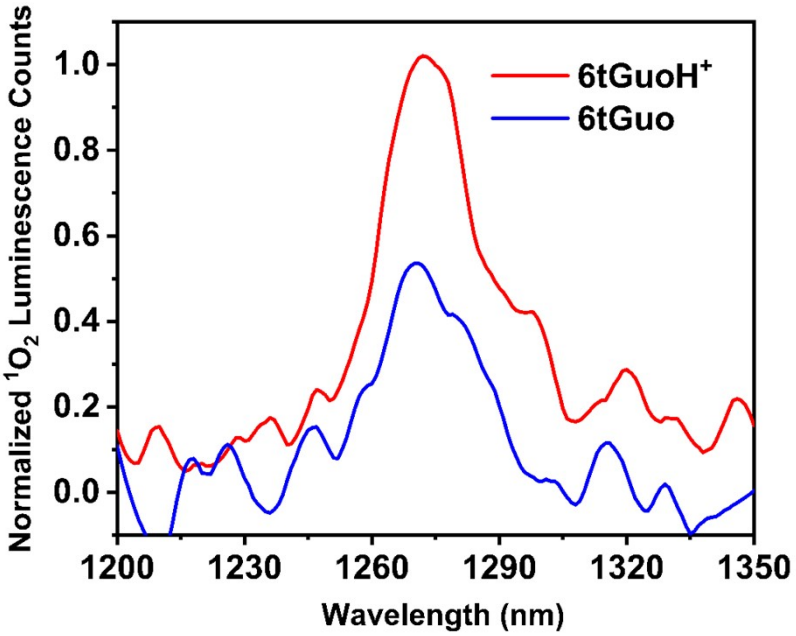

Figure S9. Singlet oxygen ($^1O_2$) phosphorescence at 1270 nm for 6tGuo and $6tGuoH^+$, both measured at $OD_{350\ nm}$ = 0.4 under air-saturated conditions with excitation at 350 nm.

S5. Optimized CASSCF Cartesian Coordinates

6tGuo

S_0

C	-1.5778284391	0.5272778470	-0.3390919322
C	-4.0046177053	0.6088798769	-0.3972217675
C	-2.5429377855	2.0124059348	1.0033426842
C	-2.7553679125	0.0535373802	-0.8497992498
C	-1.2195768509	-1.0381732151	-1.8089131494
N	-0.5779558381	-0.1859798067	-0.9350731248
N	-2.5100829596	-0.9339757984	-1.7753042302
N	-1.4237219184	1.5066976002	0.6103197242
N	-3.7593589691	1.6154831327	0.5466012695
N	-2.5599924915	3.0457108978	1.9060206237
S	-5.5245189227	0.2203510581	-0.8509428965
C	1.4189485142	0.1589256301	0.5615676400
C	0.8591577147	0.0325965826	-0.8592858080
O	1.4658939894	-1.1030477482	-1.3840213534
C	2.7178098527	-1.3684859956	-0.7495987587
C	2.8534116480	-0.3201557729	0.3554310636
C	2.7045311938	-2.8092085113	-0.2777536331
O	1.6923621397	-3.0496358796	0.6568408053
O	3.6504180035	0.7194155253	-0.1300768970
H	3.5130898519	-1.2254450922	-1.4710825708
H	0.8936865828	-0.5332299896	1.2113853751
H	3.4476582339	1.5032796009	0.3583868211
H	3.2703742316	-0.7366906628	1.2666570972
H	1.1218725708	0.9121058400	-1.4380493362
H	3.6472520554	-3.0387759371	0.2046958300
H	2.6037862545	-3.4637308382	-1.1402748151
H	0.8581994968	-3.0156847952	0.2169721140
H	-3.3147028952	3.0626144242	2.5549284874
H	-1.6754066045	3.2297420536	2.3230031705
H	-0.6684079076	-1.7069615518	-2.4320330242
O	1.4279589353	1.4497997212	1.0729942953
H	0.5327718813	1.7582413898	1.1311771424
H	-4.5647059503	2.1121170994	0.8581984033

T_1

C	-1.5893617766	0.5114470955	-0.3081411803
C	-4.0028273496	0.5625648677	-0.3402542624
C	-2.5629949767	2.0215356109	1.0171796879
C	-2.7735685482	0.0467221176	-0.8320463738
C	-1.2313805670	-1.0565378033	-1.7812443711
N	-0.5871421885	-0.2303175298	-0.8910329841
N	-2.5222517317	-0.9394802236	-1.7651445925
N	-1.4465201604	1.4797058889	0.6626017676
N	-3.7847427922	1.6582246419	0.5405476877
N	-2.5802181836	3.0782918469	1.9055487701
S	-5.4565233282	0.6183414771	-1.3557208219
C	1.4086748091	0.1152218562	0.5955263621
C	0.8448453766	-0.0025533738	-0.8241845606
O	1.4616711380	-1.1295236787	-1.3594097928
C	2.7236893292	-1.3772117469	-0.7395342593
C	2.8487078907	-0.3421645520	0.3798892586
C	2.7411077207	-2.8247245107	-0.2888790916
O	1.7379536078	-3.0988324068	0.6458144409
O	3.6320774621	0.7147861844	-0.0911781410
H	3.5110603222	-1.2089567102	-1.4645734672
H	0.8936678178	-0.5920183720	1.2374405522
H	3.4077266614	1.4909474505	0.4002894065
H	3.2737376203	-0.7664638962	1.2838701233
H	1.1028760064	0.8841743627	-1.3956287504
H	3.6900706190	-3.0440988085	0.1860786908
H	2.6484978047	-3.4677690761	-1.1611886732
H	0.8999254976	-3.0379317666	0.2158949956
H	-3.2774496940	3.0209897104	2.6158592597
H	-1.6794964691	3.2844450052	2.2770210787
H	-0.6837509755	-1.7275884894	-2.4058626083
O	1.3999663081	1.3992292264	1.1232869136
H	0.4990046997	1.6927848098	1.1872562178
H	-4.5470319502	2.2667607924	0.7299187172

T_1/S_0

C	-1.6107223415	0.5108172605	-0.3536263957
C	-4.0596106462	0.5594428668	-0.3555679453
C	-2.5668201511	1.8803818380	1.1156483368
C	-2.8144442147	0.0409160657	-0.8553278719
C	-1.2854123973	-1.0855194011	-1.8067642910
N	-0.6273556776	-0.2216399261	-0.9445194728
N	-2.5697247303	-0.9797101069	-1.7681849909
N	-1.4460638749	1.4579876158	0.6169363242
N	-3.7909586385	1.4378989971	0.7390553953
N	-2.5461312435	2.8432007479	2.0827479275
S	-4.5167979036	1.3439251236	-1.9453633810
C	1.3917700553	0.2217938431	0.4969556520
C	0.8116573170	-0.0140650179	-0.9009612510
O	1.4006789422	-1.1975077094	-1.3352829572
C	2.6700235311	-1.4043079465	-0.7139808049
C	2.8228352679	-0.2736812259	0.3050348128
C	2.6782391841	-2.8051293486	-0.1343087817
O	1.6852011438	-2.9805633946	0.8346052461
O	3.6126749269	0.7245032898	-0.2706404481
H	3.4476948550	-1.3113931544	-1.4625440680
H	0.8769364632	-0.4186832853	1.2054032090
H	3.4135527058	1.5446493395	0.1560058465
H	3.2540240801	-0.6196177297	1.2389521313
H	1.0783804063	0.8107891469	-1.5540742365
H	3.6315160794	-2.9914562492	0.3459940523
H	2.5664300720	-3.5237250989	-0.9428994270
H	0.8429577630	-2.9692024936	0.4090557088
H	-3.2990077571	2.8631233192	2.7317951630
H	-1.6519092628	3.0144936556	2.4824299601
H	-0.7385078450	-1.7679396868	-2.4194302721
O	1.4066043003	1.5471954927	0.9065075157
H	0.5079094111	1.8440044917	0.9832070082
H	-4.5756198204	1.9190186811	1.1131423053

6tGuoH$^+$

S_0

C	-1.7138390281	0.1601541703	-0.2730887055
C	-3.9094412805	-0.7928431837	0.1754968471
C	-3.3774739008	1.6012569038	-0.0684574288
C	-2.5027744908	-0.9251857358	-0.0675051163
C	-0.4543301084	-1.6272687168	-0.4078996147
N	-0.4287411695	-0.3000702411	-0.4779600573
N	-1.6805390367	-2.0330538494	-0.1564830307
N	-2.1054493527	1.4523578272	-0.2891699951
N	-4.2396958946	0.5616469471	0.1539226365
N	-3.9057875329	2.8386300498	-0.0154158018
C	1.3524130323	1.2404350800	0.3895209782
C	0.7556540386	0.5259835400	-0.8238423155
O	1.7166460239	-0.3349864798	-1.3070412913
C	2.8873228864	-0.3390281231	-0.4960128936
C	2.4306925146	0.2477560196	0.8375958475
C	3.4499916140	-1.7393069905	-0.4416300193
O	2.4896449670	-2.5981889902	0.1284566355
O	3.5027831997	0.8750355884	1.4703966245
H	0.6085613942	1.4514251596	1.1519999853
H	3.4455184943	0.7986508195	2.4084654400
H	2.0011336080	-0.5301209677	1.4590231599
H	0.4341566429	1.2305900796	-1.5746282077
H	4.3566608369	-1.7166894514	0.1557645963
H	3.7053163003	-2.0620953910	-1.4457127373
H	2.8685051360	-3.4493913033	0.2781771727
H	-5.1948023132	0.7714653456	0.3524229136
H	-4.8822237767	2.9869587284	-0.1183564238
H	-3.3049767592	3.5883836585	-0.2718242530
H	0.4068910102	-2.2529289416	-0.5224777575
O	1.9304090521	2.4038544329	-0.0944243904
H	2.6770838449	2.6303009228	0.4414595556
H	-1.9715101495	-2.9838916971	-0.0562947976
H	3.6255442154	0.3201789775	-0.9365125387
S	-4.9733440181	-2.0000141881	0.4420349832

T_1

C	-1.7089612361	0.1547433834	-0.2460282817
C	-3.8671007182	-0.7761537459	0.2730494060
C	-3.3834777927	1.6055970352	-0.0409356030
C	-2.5138758943	-0.9418707732	-0.0245869024
C	-0.4508550961	-1.6302098352	-0.4049424753
N	-0.4247331951	-0.3132671427	-0.4691285683
N	-1.6801558248	-2.0447776505	-0.1322968711
N	-2.1150530148	1.4489011139	-0.2744040247
N	-4.2542858885	0.5774539732	0.1958301064
N	-3.9105567653	2.8559182250	0.0151215065
C	1.3504664630	1.2378593193	0.3806749045
C	0.7532192142	0.5129450438	-0.8261433547
O	1.7190656493	-0.3440435728	-1.3084163597
C	2.8899004682	-0.3392333268	-0.4986384365
C	2.4312959066	0.2500647282	0.8328490371
C	3.4613979690	-1.7358221259	-0.4401818241
O	2.5085255190	-2.5995463274	0.1340738438
O	3.5037786092	0.8796264170	1.4634337377
H	0.6072178257	1.4529418680	1.1424122822
H	3.4266426074	0.8366950713	2.4023076318
H	2.0037565767	-0.5273832957	1.4561377806
H	0.4252799995	1.2115890496	-1.5797727261
H	4.3694355026	-1.7051321793	0.1548662087
H	3.7167609823	-2.0596173304	-1.4440754344
H	2.8961932421	-3.4450902764	0.2922585943
H	-5.1664789936	0.8042151607	0.5260074050
H	-4.8601422939	2.9874114388	-0.2502578304
H	-3.2907142690	3.5822837528	-0.2658385997
H	0.4049513225	-2.2583390831	-0.5392174061
O	1.9262695113	2.3992829599	-0.1119046625
H	2.6768408756	2.6267586512	0.4178644414
H	-1.9546028193	-3.0009691476	-0.0573899166
H	3.6244440522	0.3224411873	-0.9418428631
S	-5.1144484948	-2.0252725655	0.1691152546

T_1/S_0

C	-2.0088790067	-0.0925176549	-1.0980783892
C	-3.9053827144	-0.8296368038	0.2969668627
C	-3.4667456013	1.4742878364	-0.5274343500
C	-2.7312378718	-1.0995861659	-0.4641910424
C	-0.8598159477	-1.9551215227	-1.2717821328
N	-0.8543592078	-0.6637879465	-1.5944209154
N	-1.9368672661	-2.2412934184	-0.5780114285
N	-2.3275150073	1.1861808307	-1.1629204318
N	-4.2049234017	0.5715915407	0.1130044969
N	-3.8549274600	2.7571952362	-0.5284858052
C	1.1240508704	0.8796210044	-1.6268985070
C	0.1598515562	0.0128416465	-2.4381984079
O	0.9065427800	-0.9777529573	-3.0397597123
C	2.2768304046	-0.9210096812	-2.6579988922
C	2.2824846442	-0.0917691192	-1.3761292839
C	2.8178262447	-2.3256524846	-2.5362304334
O	2.0902976353	-3.0137817104	-1.5450091741
O	3.5077465560	0.5595571577	-1.2407198644
H	0.6696343152	1.2620601388	-0.7180326209
H	3.7475740645	0.6620462911	-0.3345227538
H	2.0726879476	-0.7259949491	-0.5219231985
H	-0.3812864775	0.6022132772	-3.1618721544
H	3.8697876062	-2.2619952238	-2.2740852006
H	2.7295660555	-2.8276030714	-3.4942632042
H	2.4919044594	-3.8505085736	-1.3745506475
H	-5.0333442059	0.8906948124	0.5667049586
H	-4.7478738788	3.0433203699	-0.2033380412
H	-3.3291144167	3.3941050403	-1.0810341773
H	-0.0849149626	-2.6430841443	-1.5422412448
O	1.5221711473	1.9071157430	-2.4688186953
H	2.4065788106	2.1657397720	-2.2524613249
H	-2.1877573441	-3.1537250090	-0.2584417123
H	2.8361930815	-0.3935597828	-3.4213086190
S	-4.9895938886	-1.9553101275	-0.6291432280

S6. Supplementary References

1. D. Song, W. Yang, T. Qin, L. Wu, K. Liu and H. Su, *J. Phys. Chem. Lett.*, 2014, **5**, 2259-2266.
2. Z. Lin, J. Li, C. Chen, L. Zhou, J. Jie and H. Su, *Chin. J. Chem. Phys.*, 2024, **37**, 2407098.
3. J. J. Snellenburg, S. P. Laptenok, R. Seger, K. M. Mullen and I. H. M. V. Stokkum, *J. Stat. Soft.*, 2012, **49**, 1−22.
4. I. H. van Stokkum, D. S. Larsen and R. van Grondelle, *Biochim. Biophys. Acta*, 2004, **1657**, 82-104.
5. C. Reichardt, C. Guo and C. E. Crespo-Hernández, *J. Phys. Chem. B*, 2011, **115**, 3263-3270.
6. J. D. Chai and M. Head-Gordon, *J. Chem. Phys.*, 2008, **128**, 084106.
7. P. C. Hariharan and J. A. Pople, *Theor. Chim. Acta.*, 1973, **28**, 213−222.
8. M. J. Frisch, J. A. Pople and J. S. Binkley, *J. Chem. Phys.*, 1984, **80**, 3265−3269.
9. S. Bai and M. Barbatti, *Phys. Chem. Chem. Phys.*, 2018, **20**, 16428-16436.
10. S. Liu, Y. Lee, L. Chen, J. Deng, T. Ma, M. Barbatti and S. Bai, *Phys. Chem. Chem. Phys.*, 2024, **26**, 13965-13972.
11. A. V. Marenich, C. J. Cramer and D. G. Truhlar, *J. Phys. Chem. B*, 2009, **113**, 6378-6396.
12. L. P. Quick, N. M. R. Frieler, Z. J. Devereaux, E. O. Soley, E. Israel, G. Berden, J. Martens and M. T. Rodgers, *J. Am. Soc. Mass Spectrom.*, 2025, **36**, 1120-1138.
13. M. J. Janicki, C. L. Kufner, Z. R. Todd, S. C. Kim, D. K. O'Flaherty, J. W. Szostak, J. Šponer, R. W. Góra, D. D. Sasselov and R. Szabla, *J. Phys. Chem. Lett.*, 2021, **12**, 6707-6713.
14. C. Crespo-Hernández, B. Cohen, P. Hare and B. Kohler, *Chem. Rev.*, 2004, **104**, 1977-2019.
15. X. Zhang, J. Jie, D. Song and H. Su, *J. Phys. Chem. A*, 2020, **124**, 6076-6083.
16. T. Lu and F. Chen, *J. Comput. Chem.*, 2012, **33**, 580−592.
17. M. J. Frisch, G. W. Trucks, H. B. Schlegel, G. E. Scuseria, M. A. Robb, J. R. Cheeseman, G. Scalmani, V. Barone, G. A. Petersson and H. e. a. Nakatsuji, *CT*, 2016.
18. H. J. Werner and W. Meyer, *J. Chem. Phys.*, 1980, **73**, 2342-2356.
19. B. O. Roos, P. R. Taylor and P. E. M. Sigbahn, *Chem. Phys.*, 1980, **48**, 157-173.
20. H. J. Werner and P. J. Knowles, *J. Chem. Phys.*, 1985, **82**, 5053-5063.
21. H.-J. Werner, *Mol. Phys.*, 1996, **89**, 645-661.
22. P. Celani and H.-J. Werner, *J. Chem. Phys.*, 2000, **112**, 5546-5557.
23. H.-J. Werner, P. J. Knowles, G. Knizia, F. R. Manby and M. Schütz, *WIREs Comput.Mol.Sci.*, 2012, **2**, 242-253.
24. B. Ashwood, S. Jockusch and C. E. Crespo-Hernández, *Molecules (Basel, Switzerland)*, 2017, **22**, 379.